


Improving detection efficiency of superconducting nanowire single-photon detector using multilayer antireflection coating

Cite as: AIP Advances 8, 115022 (2018); <https://doi.org/10.1063/1.5034374>

Submitted: 11 April 2018 • Accepted: 09 November 2018 • Published Online: 20 November 2018

Hao Li, Xiaoyan Yang,  Lixing You, et al.



View Online



Export Citation



CrossMark

ARTICLES YOU MAY BE INTERESTED IN

[Single-photon detectors combining high efficiency, high detection rates, and ultra-high timing resolution](#)

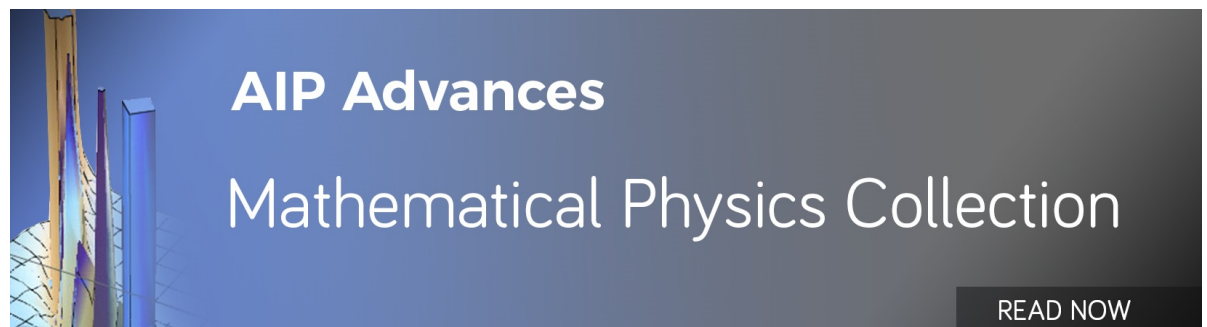
APL Photonics 2, 111301 (2017); <https://doi.org/10.1063/1.5000001>

[Picosecond superconducting single-photon optical detector](#)

Applied Physics Letters 79, 705 (2001); <https://doi.org/10.1063/1.1388868>

[NbN superconducting nanowire single-photon detector with an active area of 300 \$\mu\text{m}\$ -in-diameter](#)

AIP Advances 9, 075214 (2019); <https://doi.org/10.1063/1.5095842>



AIP Advances
Mathematical Physics Collection

READ NOW

Improving detection efficiency of superconducting nanowire single-photon detector using multilayer antireflection coating

Hao Li,^{1,2,a} Xiaoyan Yang,^{1,2,a} Lixing You,^{1,2,b} Heqing Wang,^{1,2,3} Peng Hu,^{1,2,3} Weijun Zhang,^{1,2} Zhen Wang,^{1,2} and Xiaoming Xie^{1,2}

¹State Key Laboratory of Functional Materials for Informatics, Shanghai Institute of Microsystem and Information Technology, Chinese Academy of Sciences (CAS), 865 Changning Rd., Shanghai 200050, China

²CAS Center for Excellence in Superconducting Electronics, 865 Changning Rd., Shanghai 200050, China

³University of CAS, 19A Yuquan Rd, Beijing 100049, China

(Received 11 April 2018; accepted 9 November 2018; published online 20 November 2018)

Optical cavity with backside optical coupling is one of the prevalent optical structures for superconducting nanowire single photon detector. A single layer anti-reflection coating (ARC) on the backside of the substrate is often adopted to enhance the transmittance to the substrate. We here apply a multilayer ARC to further increase the transmittance from 94.5% to 99.5%. An NbTiN SNSPD made on such a substrate with cavity structure presents a system detection efficiency of 90.1% at a dark count rate (DCR) of 100 Hz, which is the best value reported for backside optical coupled SNSPD at 1550 nm. It shows a timing jitter of ~40.7 ps and the recovery time constant of ~22.9 ns. © 2018 Author(s). All article content, except where otherwise noted, is licensed under a Creative Commons Attribution (CC BY) license (<http://creativecommons.org/licenses/by/4.0/>). <https://doi.org/10.1063/1.5034374>

I. INTRODUCTION

Superconducting nanowire single-photon detectors (SNSPDs) have undergone significant improvements and are attracting considerable attention because of their high detection efficiency (DE),^{1,2} low timing jitter,^{3,4} high count rate,^{5,6} and low dark count rate (DCR).^{7–10} These characteristics have enabled the key role in numerous impressive applications such as quantum key distribution in fiber,¹¹ space-ground laser communication,¹² depth imaging,^{13,14} and singlet oxygen luminescence detection.¹⁵

Gol'tsman et al. first demonstrated SNSPDs in 2001 by directly fabricating a nanowire on a substrate with a low absorption of incident photons.¹⁶ Since then, different schemes have been proposed to improve the absorption of SNSPDs. To date, two schemes have been mainly adopted in SNSPDs with high system detection efficiency (SDE): front-side coupled SNSPDs based on metallic¹ or dielectric mirrors² and backside coupled SNSPDs with cavity.^{17,18} Although the former set the SDE record of WSi,¹ MoSi¹⁹ or NbN SNSPD,² one existing issue is that the quality of ultra thin superconducting film might be affected by the surface quality of the post fabricated mirrors on the substrate, especially crystalline material. In comparison, the SNSPDs with cavity structure were less affected since the mirror was deposited after the fabrication of the nanowire. Unfortunately, the reported SDEs of SNSPDs with cavity structure were only about 80%.^{17,18,20} Indeed, one factor which limits SDE is the optical transmittance from the air to the substrate. Although a simple anti-reflection coating (ARC) layer has been utilized in the cavity SNSPDs,^{17,18,21} the interface optical loss due to impedance mismatch still exists and it cannot be overlooked if one wants to further increase SDE.

^aThese authors contributed equally.

^blxyou@mail.sim.ac.cn

One efficient approach to further decrease the optical loss is to use the multilayer ARC, which was applied in the mirror based SNSPDs.¹ In this study, we replaced the simple ARC with a multilayer optical film for a SNSPD with the cavity structure. The optical transmittance from air to the Si substrate was improved from 94.5% to 99.5%. The fabricated detector exhibits SDE of 90.1% at DCR of 100 Hz. The SNSPD has a timing jitter of ~ 40.7 ps, and a recovery time constant of ~ 22.9 ns.

II. DEVICE DESIGN AND FABRICATION

Figure 1 shows the structure of the proposed SNSPD, which is composed of a conventional cavity SNSPD with a multilayer ARC on its backside. The cavity SNSPD is an updated version of the cavity-structured SNSPD first introduced by Rosfjord et al.²¹ It was fabricated on a commercial double-side-oxidized Si substrate with the oxidized layer thickness of a quarter-wavelength (~ 263 nm) for both sides. The SiO_2 layer on the back side of the substrate functioned as an antireflection layer for 1550 nm wavelength radiation, and the layer at the front side served as a component of the cavity structure. The nanowires were imbedded in two optical stacks with SiO and/or SiO_2 as the dielectric materials. A metal mirror made of Ti/Au bi-layer was finally deposited on top. Two limiting factors affecting optical absorption into the SNSPD are the optical transmittance from the air to the Si substrate T_{arc} and the absorptance of the superconducting nanowire corresponding to photons incident from the substrate A_{abs} . Both a high T_{arc} and a high A_{abs} are necessary for a high-DE SNSPD. A high absorptance A_{abs} close to unity could be obtained by optimizing the geometrical size of nanowire or cavity.^{17,18} On the other hand, the simple approach for increasing T_{arc} is to use a single-layer ARC with a refractive index between the refractive indices of air and Si. The reflection loss is minimized when $n_{arc} = \sqrt{n_{Si}n_{air}}$, where n_{arc} is the index of the thin ARC layer and n_{Si} and n_{air} are the indices of the Si and air media, respectively. However, in practice, the performance of a simple one-layer coating is limited by the difficulty associated with identifying suitable materials. In a conventional cavity SNSPD, the SiO_2 layer on the back side of the substrate functions as an antireflection layer for 1550 nm wavelength radiation. The calculated transmittance T_{arc} is shown in Figure 2 which is improved from $\sim 70.0\%$ to $\sim 94.5\%$ upon the incorporation of the single layer ARC. A further reduction of the reflection loss is possible through the use of multiple coating layers that are designed such that reflections from the surfaces undergo maximum destructive interference. When two or more layers are used, an ARC with maximum reflectivity of less than 0.5% is commonly achievable. In the proposed device, the multilayer ARC was designed using the software Essential Macleod. The multilayer ARC comprised five bilayers of $\text{TiO}_2/\text{SiO}_2$. The thicknesses of each bilayer from the bottom to the top were 70.4/98.0, 180.7/266.4, 172.7/529.8, 171.7/265.7, and 171.4/264.3 nm. The calculated results indicate a 100 nm bandwidth and 99.9% transmittance as shown in

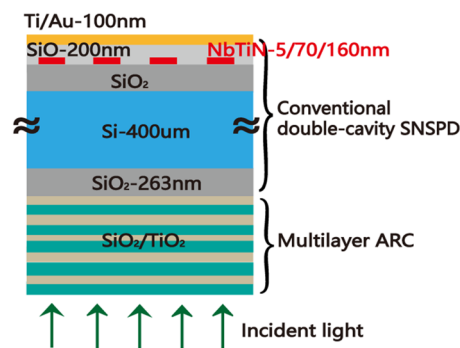


FIG. 1. Schematic of the structure of the conventional cavity SNSPD integrated with a multilayer ARC. The conventional cavity SNSPD was designed with a thermally oxidized Si substrate, superconducting nanowires imbedded in two optical stacks (SiO and/or SiO_2), and a metal mirror on top. The multilayer ARC was comprised five bilayers of $\text{TiO}_2/\text{SiO}_2$. The thicknesses of each bilayer from the bottom to the top were 70.4/98.0, 180.7/266.4, 172.7/529.8, 171.7/265.7, 171.4/264.3 nm respectively.

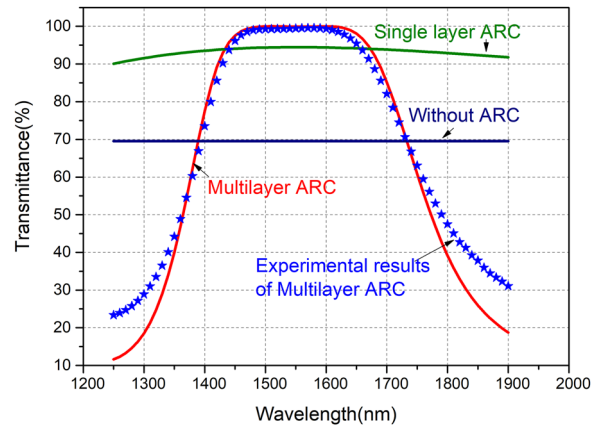


FIG. 2. Different T_{arc} with a multilayer ARC, with a single-layer ARC, and without an ARC.

Figure 2(a). Experimentally, to verify the performance of the multilayer ARC, we fabricated the same coatings on both sides of a thermally oxidized Si wafer. Then we measured the light transmittance after passing through the wafer with multilayer ARC on both sides as T_{arc}^2 . The subsequently obtained T_{arc} of the multilayer ARC is shown in Figure 2(a) with a 100 nm bandwidth and 99.5% transmittance.

We started our device fabrication with a 2 inch Si substrate that was thermally oxidized on both sides. Five periodic $\text{SiO}_2/\text{TiO}_2$ bilayers were deposited on the backside of the substrate using ion-beam-assisted deposition. Then, a 5-nm-thick NbTiN film was deposited on the front side by reactive DC magnetron sputtering in an Ar/ N_2 gas mixture under a total pressure of 0.27 Pa. The flow rates of Ar and N_2 were set to 30 sccm and 4 sccm, respectively, using mass flow controllers. The ratio of the Nb:Ti of NbTi targets was 1:1. Subsequently, the meandered nanowire covering a circular area with a diameter of 15 μm were patterned using e-beam lithography and etched using reactive-ion etching. The linewidth and the period of the nanowire were 70 and 160 nm, respectively. A 200 nm thick SiO layer was subsequently deposited on top of the nanowires; this layer served as a dielectric material for the cavity. A 5 nm/100 nm thick Ti/Au film was subsequently deposited atop the SiO layer to create a mirror for the optical cavity.

III. DEVICE MEASUREMENT AND RESULTS

The SNSPD was packaged in a copper sample mount. A lensed single-mode fiber was aligned directly from the backside of the substrate onto the SNSPD. The alignment was achieved using a homemade alignment system based on an inverted microscope, which may tune the relative position between detector and the fiber end face with an acceptable precision ($\sim 2 \mu\text{m}$ in X-Y plane and $\sim 10 \mu\text{m}$ in Z plane). The lensed fiber was specifically designed to ensure that the beam waist of the light was smaller than the size of the meander structure, and its focus was located on the plane of the nanowire. The packaged module was then mounted on the cold head of a two-stage Gifford–McMahon cryocooler with a working temperature of 2.1 K. The superconducting transition temperature T_c of SNSPD, defined as the midpoint of the resistivity–temperature transition, was measured to be 7.9 K. Outside the cryocooler, the device was connected to a room-temperature bias-tee. An isolated voltage source in series with a resistor (20 k Ω) provided a stable current bias to the detector. The bias current was fed to the device through a *dc* port of the bias-tee; high-frequency response pulses of the SNSPD were extracted from the *rf* port of the bias-tee and subsequently amplified via an ultra-wideband amplifier. The amplified pulse signals were read by an oscilloscope or counted by a photon counter. The fiber laser source was connected via two variable attenuators and a polarization controller in series.

A continuous-wave laser acting as a photon source was heavily attenuated to achieve a photon flux of 10^5 photons/s. The SDE was defined as $(\text{OPR}-\text{DCR})/\text{PR}$, where OPR is the output pulse

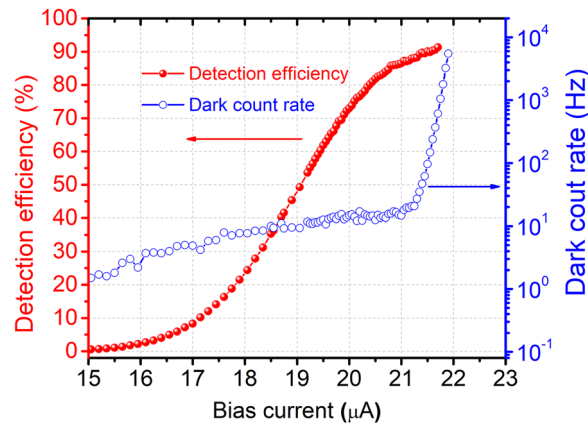


FIG. 3. SDE and DCR versus bias current for the SNSPD.

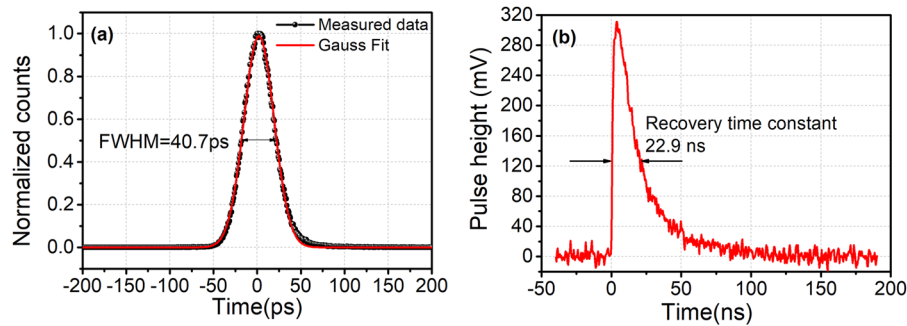


FIG. 4. (a) Histograms of the time-correlated photon counts measured at a wavelength of 1550 nm. The red lines are the curves fitted using a Gaussian distribution. (b) Oscilloscope persistence map of the response at a bias current of 21.5 μA .

rate of the SNSPD, as measured using a photon counter, DCR is the dark count rate when the laser was blocked, and PR is the total photon rate input to the system. At each bias current, an automated shutter in a variable attenuator blocked the incident photons, then the dark counts were collected for 10 seconds using the counter. When the shutter is off, the output photon counts were collected for another 10 s. The relative errors of the SDE values were estimated to be 2.82% at 1550 nm, resulting from the calibration of the laser power, as given by the power meter (2.80%, Keysight 81624B), and the incident laser power fluctuation (less than 0.30%).

Figure 3 presents the SDE and DCR relations of the bias current. SDE approaches a saturated behavior when the bias current is close to the switching current (21.7 μA). The SDE was $\sim 90.1\%$ at a DCR of 100 Hz, which is the highest value reported for the SNSPD with the cavity structure for the wavelength of 1550 nm.

The timing jitter of the SNSPD system was measured via the time-correlated single-photon counting method using a femtosecond laser at a wavelength 1550 nm.²² The timing jitter defined by the full width at half maximum value of the histogram was 40.7 ps. The measured oscilloscope trace of real-time photon response pulse is presented in Fig. 4(b). Defining the recovery time as the time width at the 1/e of the magnitude of the pulse, it gives a value of 22.9 ns.

IV. DISCUSSION AND CONCLUSIONS

In this work, an increase of $\sim 5\%$ transmittance was observed because of the nearly lossless reflection of the multilayer ARC. We then realized cavity-type NbTiN SNSPDs with multilayer ARC coatings. The fabricated SNSPDs showed a SDE of 90.1% at DCR of 100 Hz, which is the highest value reported for the SNSPD with cavity structure at 1550 nm. Due to the resonance effect on the

absorptance, we will optimize the thickness of the SiO cavity material and the geometrical parameters of the superconducting nanowire for further SDE improvement.

ACKNOWLEDGMENTS

This work was funded by the National Key R&D Program of China (2017YFA0304000), the National Natural Science Foundation of China (Grant Nos. 61501439, and 61601446), the Science and Technology Commission of Shanghai Municipality under Grant (16JC1400402), Program of Shanghai Academic/Technology Research Leader (18XD1404600) and the Joint Research Fund in Astronomy (U1631240) under cooperative agreement between the NSFC and the Chinese Academy of Sciences (CAS).

The authors declare no competing financial interests.

- ¹ F. Marsili, V. B. Verma, J. A. Stern, S. Harrington, A. E. Lita, T. Gerrits, I. Vayshenker, B. Baek, M. D. Shaw, R. P. Mirin, and S. W. Nam, *Nat. Photon.* **7**(3), 210–213 (2013).
- ² W. Zhang, L. You, H. Li, J. Huang, C. Lv, L. Zhang, X. Liu, J. Wu, Z. Wang, and X. Xie, *Sci. China Phys. Mech.* **60**(12), 120314 (2017).
- ³ J. Wu, L. You, S. Chen, H. Li, Y. He, C. Lv, Z. Wang, and X. Xie, *Appl. Opt.* **56**(8), 2195–2200 (2017).
- ⁴ I. Esmail Zadeh, J. W. N. Los, R. B. M. Gourgues, V. Steinmetz, G. Bulgarini, S. M. Dobrovolskiy, V. Zwiller, and S. N. Dorenbos, *APL Photon.* **2**(11), 111301 (2017).
- ⁵ W. H. P. Pernice, C. Schuck, O. Minaeva, M. Li, G. N. Goltsman, A. V. Sergienko, and H. X. Tang, *Nat. Commun.* **3**, 1325 (2012).
- ⁶ D. Rosenberg, A. J. Kerman, R. J. Molnar, and E. A. Dauler, *Opt. Exp.* **21**(2), 1440–1447 (2013).
- ⁷ X. Yang, H. Li, W. Zhang, L. You, L. Zhang, X. Liu, Z. Wang, W. Peng, X. Xie, and M. Jiang, *Opt. Exp.* **22**(13), 16267–16272 (2014).
- ⁸ H. Shibata, K. Shimizu, H. Takesue, and Y. Tokura, *Appl. Phys. Exp.* **6**(7), 072801 (2013).
- ⁹ C. Schuck, W. H. Pernice, and H. X. Tang, *Sci. Rep.* **3**, 1893 (2013).
- ¹⁰ W. J. Zhang, X. Y. Yang, H. Li, L. X. You, C. L. Lv, L. Zhang, C. J. Zhang, X. Y. Liu, Z. Wang, and X. M. Xie, *Supercond. Sci. Tech.* **31**(3), 035012 (2018).
- ¹¹ H. L. Yin, T. Y. Chen, Z. W. Yu, H. Liu, L. X. You, Y. H. Zhou, S. J. Chen, Y. Mao, M. Q. Huang, W. J. Zhang, H. Chen, M. J. Li, D. Nolan, F. Zhou, X. Jiang, Z. Wang, Q. Zhang, X. B. Wang, and J. W. Pan, *Phys. Rev. Lett.* **117**(19), 190501 (2016).
- ¹² D. V. Murphy, J. E. Kinsky, M. E. Grein, R. T. Schuelein, M. M. Willis, and R. E. Lafon, *Proc. SPIE* **8971**, 89710V (2014).
- ¹³ S. Chen, D. Liu, W. Zhang, L. You, Y. He, W. Zhang, X. Yang, G. Wu, M. Ren, H. Zeng, Z. Wang, X. Xie, and M. Jiang, *Appl. Opt.* **52**(14), 3241–3245 (2013).
- ¹⁴ A. McCarthy, N. J. Krichel, N. R. Gemmill, X. Ren, M. G. Tanner, S. N. Dorenbos, V. Zwiller, R. H. Hadfield, and G. S. Buller, *Opt. Exp.* **21**(7), 8904–8915 (2013).
- ¹⁵ N. R. Gemmill, A. McCarthy, B. Liu, M. G. Tanner, S. D. Dorenbos, V. Zwiller, M. S. Patterson, G. S. Buller, B. C. Wilson, and R. H. Hadfield, *Opt. Exp.* **21**(4), 5005–5013 (2014).
- ¹⁶ G. N. Gol'tsman, O. Okunev, G. Chulkova, A. Lipatov, A. Semenov, K. Smirnov, B. Voronov, A. Dzardarov, C. Williams, and R. Sobolewski, *Appl. Phys. Lett.* **79**(6), 705 (2001).
- ¹⁷ T. Yamashita, S. Miki, H. Terai, and Z. Wang, *Opt. Exp.* **21**(22), 27177–27184 (2013).
- ¹⁸ S. Miki, T. Yamashita, H. Terai, and Z. Wang, *Opt. Exp.* **21**(8), 10208–10214 (2013).
- ¹⁹ V. B. Verma, B. Korzh, F. Bussi eres, R. D. Horansky, S. D. Dyer, A. E. Lita, I. Vayshenker, F. Marsili, M. D. Shaw, H. Zbinden, R. P. Mirin, and S. W. Nam, *Opt. Exp.* **23**(26), 33792 (2015).
- ²⁰ S. Miki, M. Yabuno, T. Yamashita, and H. Terai, *Opt. Exp.* **25**(6), 6796–6804 (2017).
- ²¹ K. M. Rosfjord, J. K. W. Yang, E. A. Dauler, A. J. Kerman, V. Anant, B. M. Voronov, G. N. Gol'tsman, and K. K. Berggren, *Opt. Exp.* **14**(2), 527–534 (2006).
- ²² L. You, X. Yang, Y. He, W. Zhang, D. Liu, W. Zhang, L. Zhang, L. Zhang, X. Liu, S. Chen, Z. Wang, and X. Xie, *AIP Adv.* **3**(7), 072135 (2013).